Chen et al. *Zool. Res.* 2026, 47(3): 798−810
https://doi.org/10.24272/j.issn.2095-8137.2025.380
https://cstr.cn/32248.14.zr.2025.380

ZR | Zoological Research

Article Open Access

A *miR-305-5p*/Nerfin-1/Cyp18a1 cascade fine-tunes 20-hydroxyecdysone degradation to time pupariation in *Drosophila*

Chan Chen[1], Ze Zhang[1,*], Wei Sun[1,*]

[1] *Laboratory of Evolutionary and Functional Genomics*, *School of Life Sciences*, *Chongqing University*, *Chongqing* 401331, *China*

ABSTRACT

Steroid hormone pulses provide critical temporal signals that synchronize developmental transitions, yet the mechanisms that restrain hormone clearance and preserve pulse timing remain unclear. Using *Drosophila melanogaster* metamorphosis, a process orchestrated by 20-hydroxyecdysone (20E) pulses, this study identified Nervous fingers 1 (Nerfin-1) as a key transcriptional regulator of 20E dynamics during development. Notably, *nerfin-1* displayed stage-dependent expression in the prothoracic gland (PG) and fat body, with temporal patterns closely aligned with 20E titers. PG-specific *nerfin-1* knockdown arrested development and reduced ecdysteroid levels, whereas dietary 20E restored developmental progression. Integrated transcriptomic and chromatin immunoprecipitation analyses revealed that Nerfin-1 directly repressed *cyp18a1*, which encodes a major 20E-inactivating enzyme, thereby delaying hormone clearance during the prepupal stage. Upstream of this regulatory pathway, *miR-305-5p* acted as a post-transcriptional regulator of *nerfin-1*, showing an inverse temporal expression pattern and directly targeting the *nerfin-1* 3′ untranslated region (UTR) to suppress translation. PG-specific *miR-305-5p* overexpression reduced *nerfin-1* levels, increased *cyp18a1* expression, depleted ecdysteroid titers, and delayed development. Crucially, these phenotypes were rescued by either dietary 20E supplementation or *cyp18a1* knockdown, confirming that altered ecdysteroid degradation underlies these effects. Collectively, these findings define a novel miR-305-5p/Nerfin-1/Cyp18a1 cascade that fine-tunes hormone pulse dynamics to ensure robust developmental progression.

Keywords: Ecdysone pulse; Nerfin-1; Cyp18a1; MiR-305-5p

INTRODUCTION

Mammalian adolescence and insect metamorphosis represent critical transitions from juvenile to adult stages that culminate in sexual maturation and extensive remodeling of physiology, morphology, and behavior. These developmental programs are primarily driven by steroid hormones (Tennessen & Thummel, 2011; Terasawa & Fernandez, 2001), which act through gene-regulatory networks to control physiological and morphological transformations. However, continuous presence of these hormones can destabilize endocrine homeostasis and disrupt developmental timing. Instead, steroid hormones are typically secreted in a temporally restricted, pulsatile manner, characterized by rapid surges in blood concentration within specific developmental windows, followed by swift return to baseline levels (Terasawa & Fernandez, 2001).

In insects, metamorphosis is initiated and coordinated by ecdysteroids, the principal steroid hormones governing postembryonic developmental transitions (Andres & Thummel, 1992; Riddiford et al., 2003). At the end of the final larval instar, increasing ecdysteroid titers terminate feeding, promote gut clearance, and trigger entry into the wandering stage. During the transition to the prepupal stage, insect mobility declines, the body contracts, and ecdysteroid levels reach a peak before rapidly falling, generating a characteristic endocrine pulse. The timing, magnitude, and duration of this pulse are essential for ordering developmental events and ensuring precise progression through metamorphosis (Niwa & Niwa, 2016; Rewitz et al., 2013; Yamanaka et al., 2013).

Ecdysteroid pulse formation is closely linked to steroid biosynthesis (Warren et al., 2006). During larval development, ecdysone is primarily synthesized in the prothoracic gland (PG) from dietary cholesterol (Rewitz et al., 2009). Within the PG, a sequence of catalytic reactions, mediated by *Halloween* gene-encoded enzymes, including Neverland (*nvd*), Shroud (*sro*), Disembodied (*dib*), Spookier (*spok*), Phantom (*phm*), and Shadow (*sad*), converts phytosterols into ecdysone (Enya et al., 2014; Niwa et al., 2004, 2005, 2010; Ono et al., 2006;

Received: 06 November 2025; Accepted: 11 December 2025; Online: 12 December 2025

Foundation items: This work was supported by the National Natural Science Foundation of China (32070499), Natural Science Foundation of Chongqing (CSTB2025NSCQ-GPX0734), and Fundamental Research Funds for the Central Universities (2025CDJ-IAISYB-022)

*Corresponding authors, E-mail: zezhang@cqu.edu.cn; sunwei077@cqu.edu.cn

Yoshiyama et al., 2006). Ecdysone is subsequently converted into the active hormone 20-hydroxyecdysone (20E) by Shade (Shd) (Petryk et al., 2003). Recent studies have identified several transcription factors that directly or indirectly regulate *Halloween* gene expression, thereby influencing ecdysteroid biosynthesis and pulse initiation (Cheng et al., 2014; Kamiyama & Niwa, 2022; Komura-Kawa et al., 2015; Li et al., 2016; Liu et al., 2024; Moeller et al., 2013; Parvy et al., 2005, 2014; Uryu et al., 2018; Zeng et al., 2020). However, while pulse initiation is relatively well-studied, the mechanisms that terminate ecdysteroid pulses and drive the rapid decline in hormone titers remain poorly explored.

Ecdysteroid pulses can be attenuated at the source by suppressing hormone production in the PG. Hormone Receptor 4 (HR4) was the first transcription factor identified as a negative regulator of ecdysteroid biosynthesis and was shown to terminate low-level feeding-stage pulses through repression of the ecdysteroidogenic gene *cyp6t3* (Ou et al., 2011). The juvenile hormone-responsive transcription factor Krüppel-homolog 1 (Kr-h1) also directly binds regulatory regions of multiple *Halloween* genes and represses their expression (Liu et al., 2018; Zhang et al., 2018). In addition, prothoracicostatic neuropeptides and non-coding RNAs, including bantam and miRNA-14, inhibit ecdysteroid production by repressing steroidogenic programs (Boulan et al., 2013; He et al., 2019; Lim et al., 2020; Ohhara et al., 2015; Yamanaka et al., 2005). While these mechanisms limit new hormone synthesis, rapid pulse termination also requires removal of existing ecdysteroids. This catabolic step is mediated in part by Cyp18a1, a cytochrome P450 enzyme that inactivates ecdysone and 20E through 26-hydroxylation (Guittard et al., 2011; Lafont et al., 2005; Rewitz et al., 2010). Cyp18a1 is broadly expressed in 20E-responsive tissues, including the PG, fat body, and midgut, and altered *cyp18a1* expression disrupts ecdysteroid homeostasis and impairs metamorphic progression (Guittard et al., 2011; Rewitz et al., 2010). Thus, termination of steroid hormone pulses depends not only on repression of biosynthetic genes but also on precise transcriptional control of catabolic enzymes such as *cyp18a1*.

In this study, Nervous fingers 1 (Nerfin-1), the *Drosophila* ortholog of human Insulinoma-associated protein 1 (INSM1), was identified as an essential regulator of insect metamorphosis. Nerfin-1 belongs to an evolutionarily conserved family of C2H2-type zinc finger transcription factors and has been characterized across diverse metazoans as a major determinant of neuronal fate commitment, differentiation, and maintenance (Farkas et al., 2008; Froldi et al., 2015; Vissers et al., 2018; Xu et al., 2017). In *D. melanogaster*, Nerfin-1 primarily functions as a sequence-specific transcriptional corepressor. It physically interacts with the TEA DNA-binding domain of the transcription factor Scalloped (Sd), a core component of the Hippo pathway effector complex, and recruits histone deacetylases (HDACs) to promote local chromatin condensation and repress genes involved in cell proliferation and alternative differentiation states (Guo et al., 2019). This study revealed a previously unknown endocrine function for Nerfin-1 in *Drosophila* metamorphosis. Notably, Nerfin-1 repressed *cyp18a1* expression, thereby restraining ecdysteroid degradation and shaping hormone pulse timing and amplitude during developmental progression. Furthermore, *miR-305-5p* acted upstream by repressing *nerfin-1* post-transcriptionally, which increased *cyp18a1* expression and promoted ecdysteroid clearance. Together, these findings define a *miR-305-5p*/Nerfin-1/Cyp18a1 regulatory cascade that controls ecdysteroid degradation, preserves ecdysteroid pulse dynamics, and ensures proper temporal coordination of metamorphic development, whereas disruption of this pathway perturbs hormone homeostasis and induces developmental defects.

MATERIALS AND METHODS

Drosophila feeding

All *Drosophila* stocks used in this study are listed in Supplementary Table S1. Flies were maintained under laboratory conditions (25°C, 60% relative humidity, 12 h light:12 h dark cycle). For pupation-timing experiments, eggs were collected on grape juice plates. Plates were prepared by boiling 5 g of agar in 100 mL of pure water, cooling to 60°C, adding 50 mL of grape juice, and dispensing 1 mL aliquots onto microscope slides. For developmental staging experiments, mated adult female flies were allowed to oviposit for 2 h in collection vials containing grape juice-coated plates and were then transferred to fresh vials. Newly hatched larvae were transferred into new vials containing cornmeal medium, and developmental status was recorded every 12 h. Each experiment was conducted in triplicate, with 30 larvae per group. Cornmeal medium was prepared by boiling 40 g of yeast powder, 100 g of glucose, 10 g of agar powder, and 90 g of cornmeal in 1 L of pure water. After cooling the mixture to 60°C, 3 mL of propionic acid and 3.5 mL of 10% butyl paraben (w/v) were added before the medium was dispensed into *Drosophila* vials.

Total RNA extraction

Larvae were collected at designated developmental time points, and the required tissues were dissected. Total RNA was extracted from dissected tissues using an RNeasy Micro Kit (Qiagen, Germany) according to the manufacturer's protocols. RNA concentration was quantified using a NanoDrop One spectrophotometer (Thermo Scientific, USA). Each experimental group included three biological replicates.

cDNA synthesis and quantitative PCR (qPCR)

For cDNA synthesis, 1 μg of total RNA was reverse transcribed into cDNA using the TransGen Biotech Reverse Transcription Kit (TransGen Biotech, China). qPCR was performed using a QuantiTect SYBR Green PCR Kit (Qiagen, Germany) according to the manufacturer's instructions. Each sample had at least three biological replicates. Primer sequences for *E75*, *EcR*, and *DHR3* were obtained from Petryk et al. (2003), and primers for *DHR4* were obtained from Ou et al. (2011). Primers for *nerfin-1, cyp18a1* and *Halloween* genes are listed in Supplementary Table S2. For mature miRNA quantification, first-strand cDNA was synthesized using the poly(A) tailing method according to the protocol provided by the manufacturer (Sangon Biotech, China). miRNA qPCR was performed using a SYBR Green qPCR Kit (Sangon Biotech, China) according to the manufacturer's instructions. U6 snRNA was used as the reference gene for miRNA expression analysis. Primers used for miRNA qPCR are listed in Supplementary Table S2.

Immunofluorescence

PGs and fat bodies were dissected from larvae at 120 h after egg laying (AEL) under a stereomicroscope. Tissues were fixed in 4% paraformaldehyde (pH 7.4) at 26°C for 25 min and washed three times for 10 min each with phosphate-buffered

saline (PBS) containing 0.3% Triton X-100 (PBST). Samples were blocked in PBST containing 2% bovine serum albumin (BSA) on a horizontal shaker at room temperature for 90 min and then incubated with primary antibodies overnight at 4°C. After three washes with PBST, samples were incubated with species-specific fluorescently labeled secondary antibodies and 4',6-diamidino-2-phenylindole (DAPI, Beyotime, China) for 2 h at room temperature in the dark. Samples were then washed three times for 10 min each in PBS, mounted in antifade mounting medium, and imaged using a Leica TCS SP8 confocal microscope.

The following antibodies were used at the indicated dilutions: anti-Dib (1:500; Ryusuke Niwa, University of Tsukuba, Japan) and anti-Nerfin-1 (1:100) (Xu et al., 2017). Alexa Fluor 488-conjugated secondary antibody (Invitrogen, USA) and Alexa Fluor 555-conjugated secondary antibody (Beyotime, China) were used for primary antibody detection.

Western blot analysis

To assess Nerfin-1 protein expression, PGs were dissected from *Phm-gal4*>+ and *Phm-gal4>UAS-nerfin-1-i* larvae at 120 h AEL. Total protein was extracted using cell lysis buffer for western blotting (Beyotime, China). Following separation by sodium dodecyl sulfate-polyacrylamide gel electrophoresis (SDS-PAGE), gel regions containing target protein bands were excised, and proteins were transferred onto polyvinylidene fluoride (PVDF) membranes at a constant current of 200 mA for 1 h. Membranes were subsequently rinsed in Tris-buffered saline containing 0.1% Tween-20 (TBST) for 5 min, and blocked in TBST containing 5% skim milk powder on a horizontal shaker at 26°C for 1.5 h. Prior to primary antibody incubation, membranes were washed three times with TBST (10 min per wash), immersed in anti-Nerfin-1 or anti-Tubulin antibody prepared in blocking buffer (1:4 000), and incubated on a shaker at 26°C for 2 h. After three additional washes with TBST, membranes were incubated with species-specific horseradish peroxidase (HRP)-conjugated secondary antibody diluted in TBST (1:6 000) for 2 h at 26°C. After three final washes with TBST (10 min each), membranes were evenly coated with ECL chemiluminescent substrate reagent (Sangon Biotech, China), incubated for 5 min in the dark at 26°C, and imaged using a chemiluminescence imaging system (Bio-Rad ChemiDoc, USA).

RNA sequencing (RNA-seq)

PGs were dissected from *Phm-gal4*>+ and *Phm-gal4>UAS-nerfin-1-i* larvae at 120 h AEL, with three biological replicates prepared for each genotype. Total RNA was extracted using an RNeasy Mini Kit (Qiagen, Germany) according to the manufacturer's instructions. Purified RNA samples were submitted to a commercial sequencing facility for paired-end sequencing on the Illumina NovaSeq 6000 platform (USA). Raw sequencing reads were processed for quality control using Trimmomatic (Sewe et al., 2022). Clean reads were aligned to the *D. melanogaster* reference genome (BDGP6.32) using HISAT2, and transcript abundance was quantified using StringTie (Pertea et al., 2016). Differential gene expression analysis was performed using DESeq2 (v.1.38.3) (Love et al., 2014). Gene Ontology (GO) enrichment analyses were conducted using the DAVID bioinformatics platform (Sherman et al., 2022).

20E administration

Synchronized *Drosophila* larvae were collected at 72 h AEL and randomly allocated to medium containing ethanol or 0.1 mg/g 20E (Sangon Biotech, China). Each vial contained 30 larvae. Developmental progression was monitored daily, and pupariation timing, eclosion rate, and adult viability were quantified.

Ecdysteroid quantification by liquid chromatography-tandem mass spectrometry (LC-MS/MS)

Third-instar *Drosophila* larvae were collected at 120 h AEL, with at least 60 larvae used per group. Three biological replicates were prepared for each group. For each replicate, hemolymph (30 μL) was collected using microcapillary puncture and immediately transferred to a prechilled 1.5 mL microcentrifuge tube. Prechilled methanol (270 μL) was added to each hemolymph sample, followed by vortex mixing for 10 s and incubation at 4°C for 10 min to precipitate proteins. Samples were centrifuged at 14 000 ×*g* for 5 min at 4°C using an Eppendorf 5424R centrifuge. The supernatant was collected, transferred to a new microcentrifuge tube, and submitted to the Analytical and Testing Center of Chongqing University for LC-MS/MS analysis. LC-MS/MS parameters were consistent with those reported previously (Xue et al., 2025).

Chromatin immunoprecipitation assay (ChIP)

Nerfin-1-mediated transcriptional repression of *cyp18a1* was observed in both the PG and fat body. Because the extremely small size of the PG limited recovery of sufficient material for ChIP, fat body tissue was used to validate Nerfin-1 binding to the *cyp18a1* regulatory region. *Drosophila* fat bodies were dissected and washed in ice-cold PBS to remove residual hemolymph. ChIP was subsequently performed using a Sonication ChIP Kit (ABclonal, China) according to the manufacturer's protocols. To identify potential Nerfin-1 binding sites, the 2 000 bp sequence upstream of the *cyp18a1* transcription start site was retrieved from FlyBase and screened against INSM1 (ortholog to Nerfin-1 in humans) in the JASPAR database (v2022). Primers were then designed to amplify the predicted binding-site-containing region. qPCR was performed to determine whether the predicted binding site was specifically enriched after immunoprecipitation. The primers used for qPCR are listed in Supplementary Table S2.

Prediction and screening of miRNAs

Candidate miRNAs targeting the *nerfin-1* 3′ UTR were predicted using the TargetScanFly v.7.2 database (Agarwal et al., 2018). Candidate selection was refined by intersecting the predicted miRNAs with the 20 most highly expressed miRNAs in the ring gland, as reported previously (Zhang et al., 2021). Statistical correlations between candidate miRNA expression levels and *nerfin-1* expression levels, both determined by qPCR, were then calculated using Pearson correlation analysis. A statistically significant negative correlation with *nerfin-1* expression was used as the screening criterion because inverse expression is consistent with miRNA-mediated suppression of target gene expression.

***In vitro* luciferase assays**

All reporter plasmids were purified using an EndoFree Plasmid Kit (Qiagen, Germany). HEK293T cells were seeded in 48-well plates and transfected with 1 000 ng of reporter plasmid complexed with polyethylenimine (Invitrogen, USA) according to the manufacturer's instructions. At 24 h post-transfection, dual-luciferase activity was quantified using the Dual-Luciferase® Reporter Assay System (Promega, USA).

Relative luciferase activity was calculated as the ratio of firefly luciferase luminescence to *Renilla* luciferase luminescence. Three independent biological replicates were performed.

Statistical analysis

All statistical analyses were performed in R using Student's *t*-test.

RESULTS

Nerfin-1 regulates *Drosophila* development by modulating ecdysteroid titers

Nerfin-1 is a highly conserved zinc finger transcription factor with established roles in neural development across various metazoans, including *Caenorhabditis elegans*, *D. melanogaster*, and mammals (Farkas et al., 2008; Vissers et al., 2018; Wu et al., 2001; Xu et al., 2017). A previous genome-wide RNAi screen in the PG revealed that PG-specific loss of *nerfin-1* delayed larval development and postponed pupariation (Danielsen et al., 2016), suggesting that *nerfin-1* may have an endocrine function in this steroidogenic tissue beyond its known function in the nervous system. Immunostaining confirmed that Nerfin-1 was expressed in PG cells and localized to the nucleus (Figure 1A). During development, *nerfin-1* expression in the PG increased progressively from the feeding to the wandering stage of third-instar larvae, peaked at the onset of the prepupal stage, and then declined (Figure 1B). This temporal profile closely paralleled fluctuations in ecdysteroid titers,

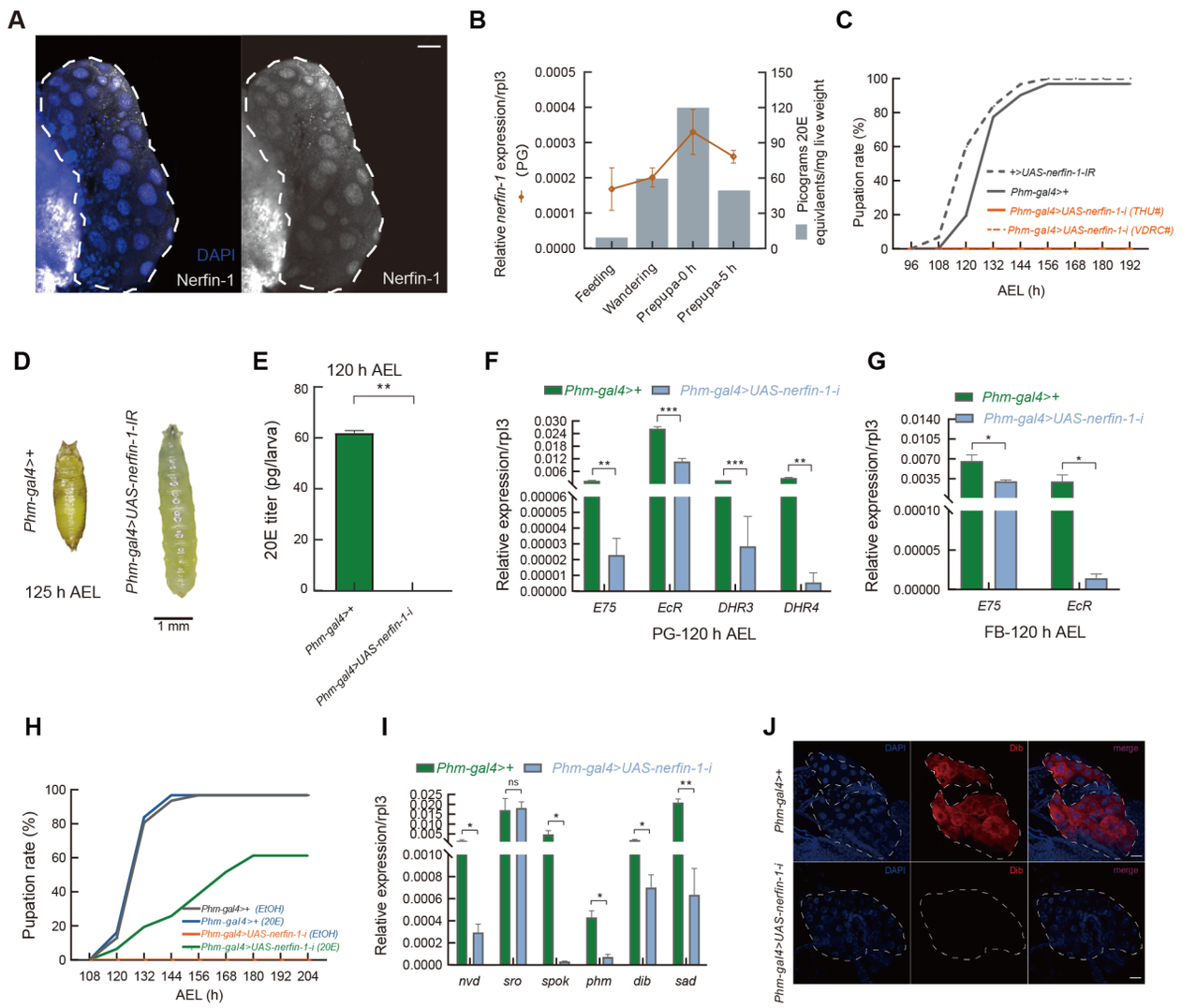

Figure 1 Nerfin-1 regulates ecdysteroid titers to control pupariation in *Drosophila*

A: Localization of Nerfin-1 protein in prothoracic gland (PG) cells dissected from W^{1118} larvae at the wandering stage. DAPI was used to stain nuclei. Scale bar: 50 μm. B: Temporal expression profile of *nerfin-1* in the ring gland dissected from W^{1118} individuals at specific developmental stages (red line). Bar chart presents developmental changes in hemolymph ecdysteroid titers based on previous data (Hodgetts et al., 1977). C: Pupation ratio of control and *nerfin-1* RNAi individuals. Two *UAS-nerfin-1-i* lines were used in (C). VDRC: Vienna *Drosophila* Resource Center; THFC: TsingHua Fly Center. VDRC lines were used to perform other experiments. D: Phenotype of *nerfin-1* RNAi at 125 h after egg laying (AEL). Scale bar: 1 mm. E: 20E concentrations in control (*Phm-gal4>+*) and *nerfin-1* RNAi (*Phm-gal4>UAS-nerfin-1-i*) larvae at 120 h AEL. F: Expression of hormone-responsive genes (ecdysone-inducible gene 75, *E75*; ecdysone receptor, *EcR*; hormone receptor 3, *DHR3*; *DHR4*) in the ring gland of control and *nerfin-1* RNAi larvae at 120 h AEL. G: Expression of hormone-responsive genes in fat bodies from control and *nerfin-1* RNAi larvae at 120 h AEL. H: Effect of 20E and ethanol (EtOH) administration on development of control and *nerfin-1* RNAi larvae. I: Expression of *Halloween* genes in control and *nerfin-1* RNAi larvae at 120 h AEL. J: Immunostaining analysis of Dib and DAPI in PG cells of control and *nerfin-1* RNAi larvae at 120 h AEL. Scale bar: 50 μm. Significance was calculated using Student's *t*-test (ns: Not significant; *: $P<0.05$; **: $P<0.01$; ***: $P<0.001$).

indicating a potential role for *nerfin-1* in endocrine regulation (Figure 1B) (Hodgetts et al., 1977).

To determine whether *nerfin-1* regulates PG function, *nerfin-1* was knocked down specifically in the PG using *Phm*-gal4. In RNAi larvae, *nerfin-1* mRNA and Nerfin-1 protein levels were both significantly reduced (Supplementary Figure S1A, B). PG-specific *nerfin-1* knockdown resulted in developmental arrest at the third-instar stage, with affected larvae failing to pupariate (Figure 1C, D). As pupariation depends on high ecdysteroid output from the PG, this phenotype implied a role for *nerfin-1* in regulating ecdysteroid concentration. Indeed, ecdysteroid titers were markedly reduced in *nerfin-1* RNAi larvae (Figure 1E). Correspondingly, expression of ecdysone-responsive genes, such as ecdysone receptor (*EcR*), hormone receptor 3 (*Hr3*), *Hr4*, and ecdysone-inducible gene 75 (*E75*), was also significantly down-regulated in both the PG (Figure 1F) and fat body (Figure 1G) of RNAi larvae. Importantly, dietary supplementation with 20E rescued developmental arrest in more than 60% of *nerfin-1* RNAi larvae and restored pupariation (Figure 1H). These findings indicate that loss of *nerfin-1* in the PG disrupts ecdysteroid homeostasis and impairs larval-to-pupal transition. Given that ecdysteroid titers are tightly controlled by steroidogenic enzyme expression, transcription of *Halloween* genes was further examined, with several shown to be significantly down-regulated upon *nerfin-1* knockdown (Figure 1I, J), supporting a role for Nerfin-1 in maintaining ecdysteroid biosynthesis.

Collectively, these results suggest that Nerfin-1 plays a critical role in regulating ecdysteroid concentration, thereby influencing larval development and metamorphic progression.

Identification of Nerfin-1 target genes in *Drosophila* metamorphosis

To define the transcriptional program regulated by Nerfin-1 during metamorphosis, RNA-seq was performed using ring glands isolated from PG-specific *nerfin-1* RNAi larvae. Given that *nerfin-1* expression increased during the wandering stage and *nerfin-1* RNAi larvae did not exhibit normal wandering behavior, control larvae at 84 h after hatching (hAH), corresponding to the wandering stage, were selected for transcriptomic comparison. PG-specific *nerfin-1* knockdown resulted in 2 113 differentially expressed genes (DEGs) relative to controls. To prioritize genes with stronger transcriptional responses, DEGs were filtered using a fold-change threshold of ≥4, yielding 579 up-regulated and 321 down-regulated genes (Figure 2A). The predominance of up-regulated genes after *nerfin-1* depletion is consistent with previous evidence indicating that Nerfin-1 functions mainly as a transcriptional repressor (Guo et al., 2019).

GO enrichment analysis using DAVID revealed that down-regulated genes were significantly enriched in 11 annotation clusters containing functionally related GO terms (Figure 2B, lower panel; Supplementary Table S3). Among these clusters, the term “regulation of hormone levels” (GO:0010817, FDR=0.022) was closely associated with ecdysone biosynthesis and included *Halloween* genes, such as *dib* and *sad*, as well as transcription factors, including *Knirps* (*Kni*) and Ecdysone-induced protein 75B (*E75B*) (Figure 2C). Genes up-regulated after PG-specific *nerfin-1* knockdown were enriched in 20 annotation clusters (Figure 2B, upper panel; Supplementary Table S4). Notably, the term “hormone metabolic process” (GO:0042445, FDR=0.016) clustered with “regulation of hormone levels”, and the two terms contained largely overlapping gene sets (Supplementary Table S4). Because this annotation group was linked to ecdysone metabolism and regulation, DEGs within “hormone metabolic process” were examined further. This analysis identified *cyp18a1*, shade (*shd*), and adipokinetic hormone (*akh*), together with juvenile hormone-associated genes, such as *cyp6t3*, juvenile hormone epoxide hydrolase 2 (*jheh2*), and *jheh3* (Figure 2C).

Previous studies have shown that Nerfin-1 acts as a transcriptional repressor in the nervous system (Guo et al., 2019; Vissers et al., 2018). Consistent with this regulatory mode, PG-specific *nerfin-1* knockdown produced an approximately 20-fold increase in *cyp18a1* expression, as validated by both RNA-seq and qPCR (Figure 2D). Ectopic *cyp18a1* overexpression in the PG recapitulated the *nerfin-1* RNAi phenotype and caused developmental arrest (Supplementary Figure S2A). Conversely, ubiquitous *nerfin-1* overexpression driven by *tubulin-gal4* produced developmental phenotypes resembling those induced by whole-body *cyp18a1* RNAi (Supplementary Figure S2B). Moreover, JASPAR-based motif analysis identified putative Nerfin-1 binding sites in the regulatory region of *cyp18a1*, suggesting direct transcriptional repression of *cyp18a1* by Nerfin-1 (Figure 3E).

Nerfin-1 controls ecdysteroid titers and metamorphosis by repressing *cyp18a1*

To define their regulatory relationship, the temporal expression patterns of *nerfin-1* and *cyp18a1* were first examined. In the PG, *cyp18a1* expression remained low during the wandering stage and at the white prepupal stage, when ecdysteroid titers were high, but increased rapidly at 5 h post-prepupal transition, coinciding with the decline in hormone titers (Figure 3A; Figure 1B). Given that Cyp18a1 regulates ecdysteroid metabolism in multiple tissues (Guittard et al., 2011), *cyp18a1* and *nerfin-1* expression were also assessed in the fat body, a major ecdysteroid-responsive tissue. Immunostaining confirmed nuclear localization of Nerfin-1 protein in fat body cells (Figure 3B). Temporal analysis further revealed that *cyp18a1* expression was inversely correlated with both ecdysteroid titers and *nerfin-1* expression, consistent with the pattern observed in the PG (Figure 3B). Functional analysis using the fat body driver Cg-gal4 showed that fat body-specific nerfin-1 knockdown significantly increased cyp18a1 expression, as observed in the PG, although no overt developmental defects were detected after fat body-specific nerfin-1 RNAi (Supplementary Figure S3).. These results suggest that Nerfin-1-mediated repression of *cyp18a1* operates across multiple ecdysteroid-regulated tissues. Consistent with direct transcriptional control, ChIP confirmed that Nerfin-1 directly bound the *cyp18a1* regulatory region containing a GGGG motif (Figure 3C) (Zhou et al., 2025).

To test the functional importance of this regulatory axis *in vivo*, *cyp18a1* was knocked down in the *nerfin-1* RNAi background. Compared with *nerfin-1* RNAi alone, combined *nerfin-1* and *cyp18a1* RNAi significantly reduced *cyp18a1* expression in the PG (Figure 3D). More importantly, 20E concentrations were markedly restored, demonstrating that the steroidogenic capacity of the PG remained largely intact after *nerfin-1* depletion and that the hormonal defect resulted primarily from *cyp18a1* derepression (Figure 3E). Consistently, *cyp18a1* knockdown rescued metamorphic progression in approximately 40% of *nerfin-1* RNAi individuals and enabled successful pupariation (Figure 3F). Collectively,

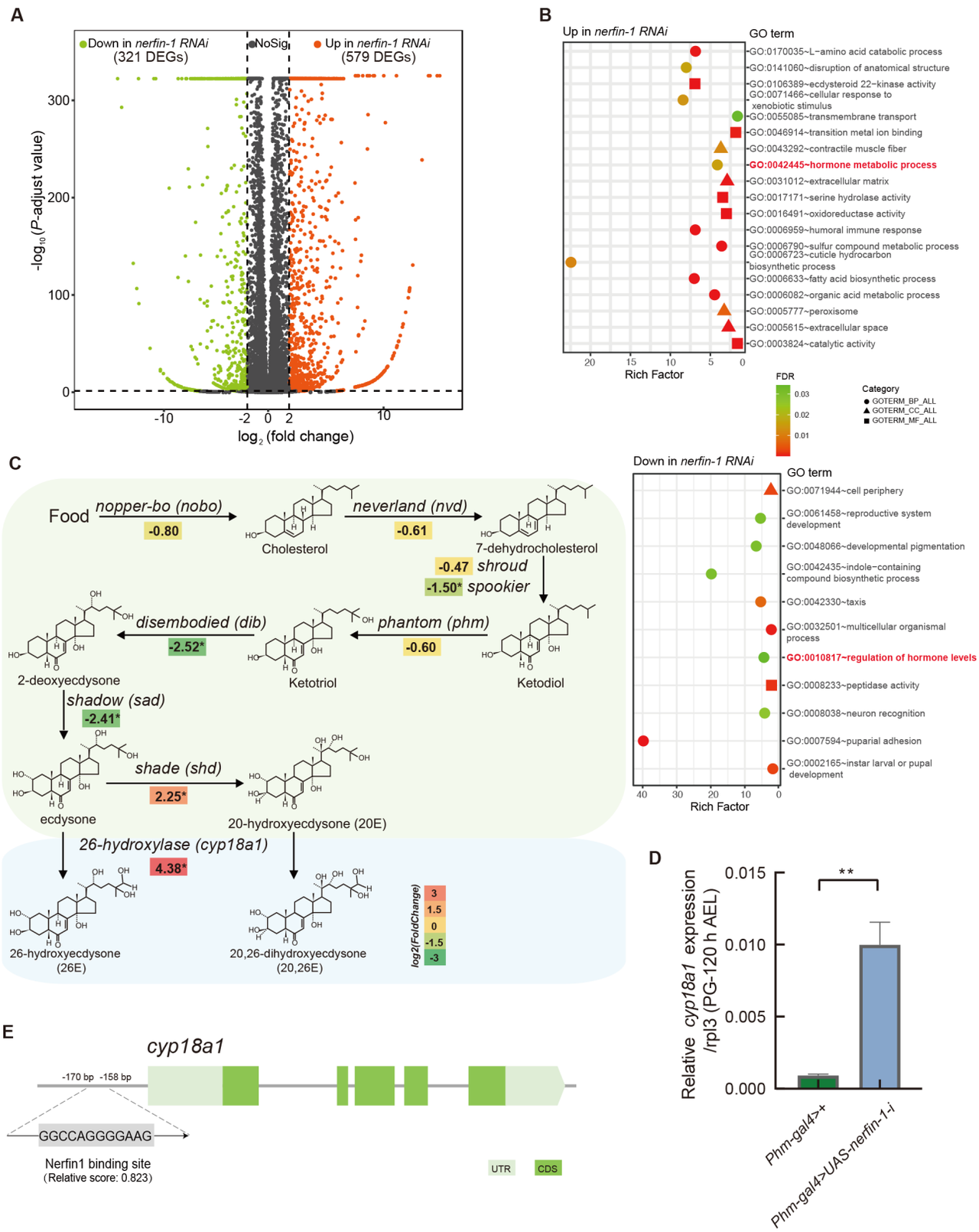

Figure 2 Transcriptome-based identification of Nerfin-1 target genes

A: Volcano plot showing differentially expressed genes (DEGs) between ring glands from control (*Phm-gal4*>+) and *nerfin-1* RNAi (*Phm-gal4>UAS-nerfin-1-i*) larvae at 120 h after egg laying (AEL). Dashed lines indicate thresholds set for differential expression, defined as $\log_2$(fold change)<−2 or >2 and adjusted *P*<0.05. Green and red dots represent significantly down-regulated and up-regulated genes in *nerfin-1* RNAi larvae, respectively, while gray dots indicate genes without significant differential expression. B: GO enrichment analysis of up-regulated genes (upper panel) and down-regulated genes (lower panel) in *nerfin-1* RNAi larvae. Hormone-related GO terms are highlighted in red. C: Fold changes in expression of genes involved in ecdysteroid biosynthesis and degradation pathways. Asterisks indicate significant DEGs. D: qPCR analysis of *cyp18a1* expression in PG cells from control and *nerfin-1* RNAi larvae at 120 h AEL. E: Predicted Nerfin-1 binding motif in the *cyp18a1* regulatory region, inferred from the human ortholog INSM1 in JASPAR (accession number: MA0155.1). Significance was calculated using Student's *t*-test (**: *P*<0.01).

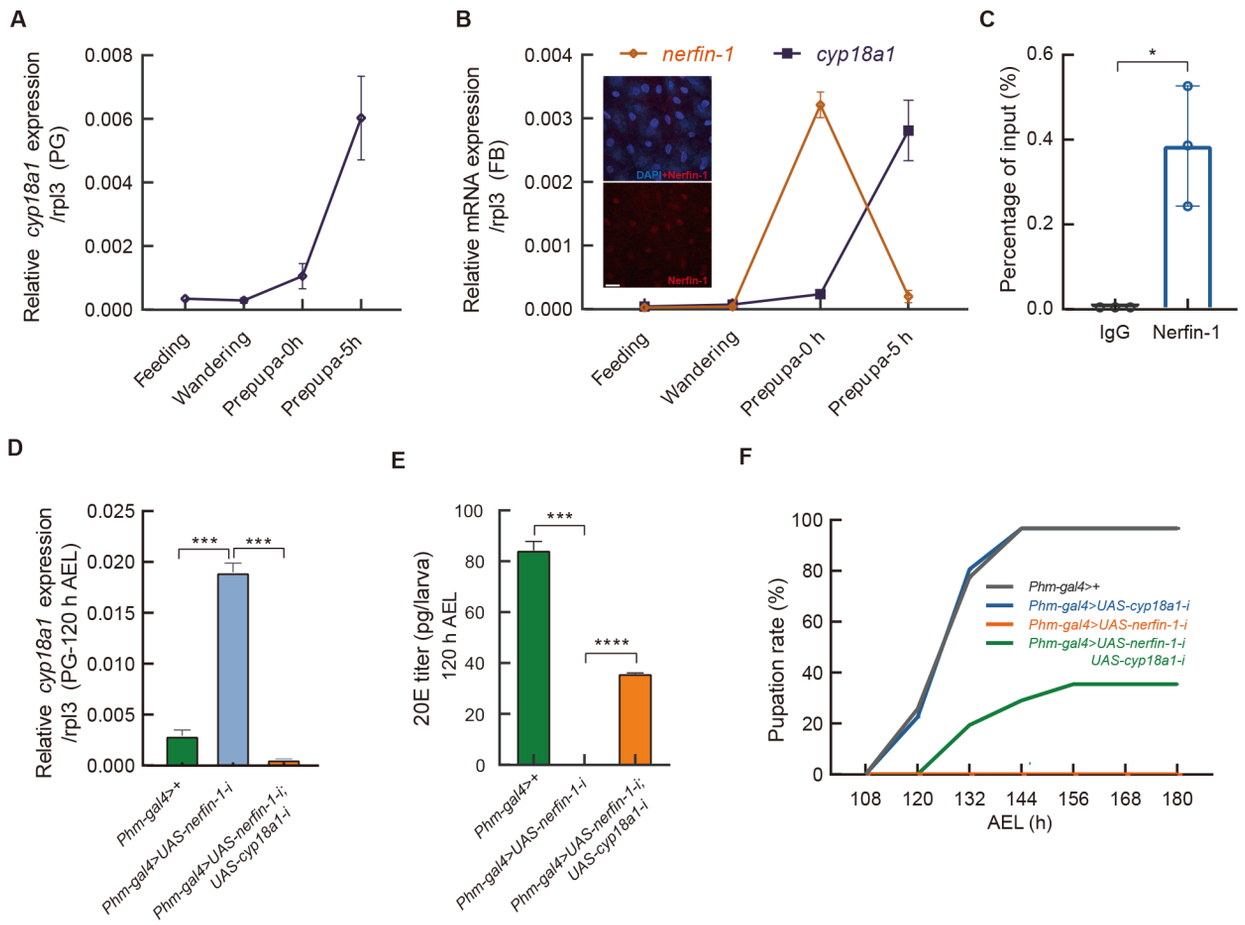

Figure 3 Nerfin-1 represses *cyp18a1* expression to maintain 20E levels

A: Temporal expression profile of *cyp18a1* in ring glands dissected from W^{1118} individuals at specific developmental stages. B: Temporal expression profiles of *nerfin-1* (red line) and *cyp18a1* (black line) in fat bodies dissected from W^{1118} individuals at specific developmental stages. Insets show immunostaining of Nerfin-1 protein and DAPI in fat bodies from W^{1118} individuals at 120 h after egg laying (AEL). C: ChIP assay confirming direct binding of Nerfin-1 to the *cyp18a1* regulatory region. IgG was used as the control. D: Expression of *cyp18a1* in ring glands from control (*Phm-gal4>+*), *nerfin-1* RNAi (*Phm-gal4>UAS-nerfin-1-i*), and rescued (*Phm-gal4>UAS-nerfin-1-i; UAS-cyp18a1-i*) larvae at 120 h AEL. E: 20E concentration in *nerfin-1* RNAi and rescued larvae. F: Pupation ratios of *nerfin-1* RNAi and rescued larvae. Significance was calculated using Student's *t*-test (*: P<0.05; ***: P<0.001; ****: P<0.0001).

these results identify Cyp18a1 as a major downstream target through which Nerfin-1 maintains 20E homeostasis and support the existence of a multi-tissue regulatory mechanism that stabilizes endocrine timing during metamorphosis.

MiR-305-5p modulates *Drosophila* development by regulating *nerfin-1* and ecdysone pulses

Given the importance of dynamic *nerfin-1* expression in ecdysone regulation, the upstream mechanism controlling *nerfin-1* expression was examined. Previous research has shown that miRNAs regulate *nerfin-1* post-transcriptionally during neurogenesis (Kuzin et al., 2007). TargetScanFly analysis identified multiple miRNA-binding sites within the *nerfin-1* 3′ UTR (Figure 4A). Integration of these predictions with the 20 most highly expressed miRNAs previously reported in the ring gland (Zhang et al., 2021), a composite endocrine structure comprising the corpora allata, corpora cardiaca, and the larger PG, identified *miR-1-3p*, *miR-9a-3p*, *miR-9a-5p*, and *miR-305-5p* as candidate post-transcriptional regulators of *nerfin-1* (Figure 4A). To evaluate these candidates, qRT-PCR was used to determine miRNA expression patterns in the PG across developmental stages, followed by correlation analysis with *nerfin-1* expression. Among the tested miRNAs, only *miR-305-5p* exhibited a significant negative correlation with *nerfin-1* expression (Pearson correlation r=−0.92, P=2.15e-5) (Figure 4B). Notably, *miR-305-5p* expression was relatively high during the feeding stage, declined sharply at the wandering stage, reached the lowest level at the white prepupal stage, and then increased again approximately 5 h after puparium formation. *miR-305-5p* is highly conserved across metazoans and has been shown to regulate adaptive intestinal homeostasis in *Drosophila* by altering Notch and insulin signaling (Figure 4C) (Foronda et al., 2014). To validate the regulatory interaction between *miR-305-5p* and *nerfin-1*, a luciferase reporter containing the *nerfin-1* 3′ UTR was constructed and expressed in HEK293T cells (Figure 4D). Overexpression of *miR-305-5p* significantly suppressed luciferase activity, whereas mutation of the predicted *miR-305-5p* seed-binding site abolished this repression (Figure 4E). These results indicate that *nerfin-1* is a direct target of *miR-305-5p*. *In vivo*, PG-specific *miR-305-5p* overexpression reduced *nerfin-1* expression, whereas inhibition of *miR-305-5p* using sponge constructs increased *nerfin-1* levels (Figure 4F–H). Together, these findings demonstrate that *miR-305-5p* suppresses *nerfin-1* expression post-transcriptionally in the PG.

Whether *miR-305-5p* regulates hormonal homeostasis through the Nerfin-1/Cyp18a1 axis was next examined. PG-

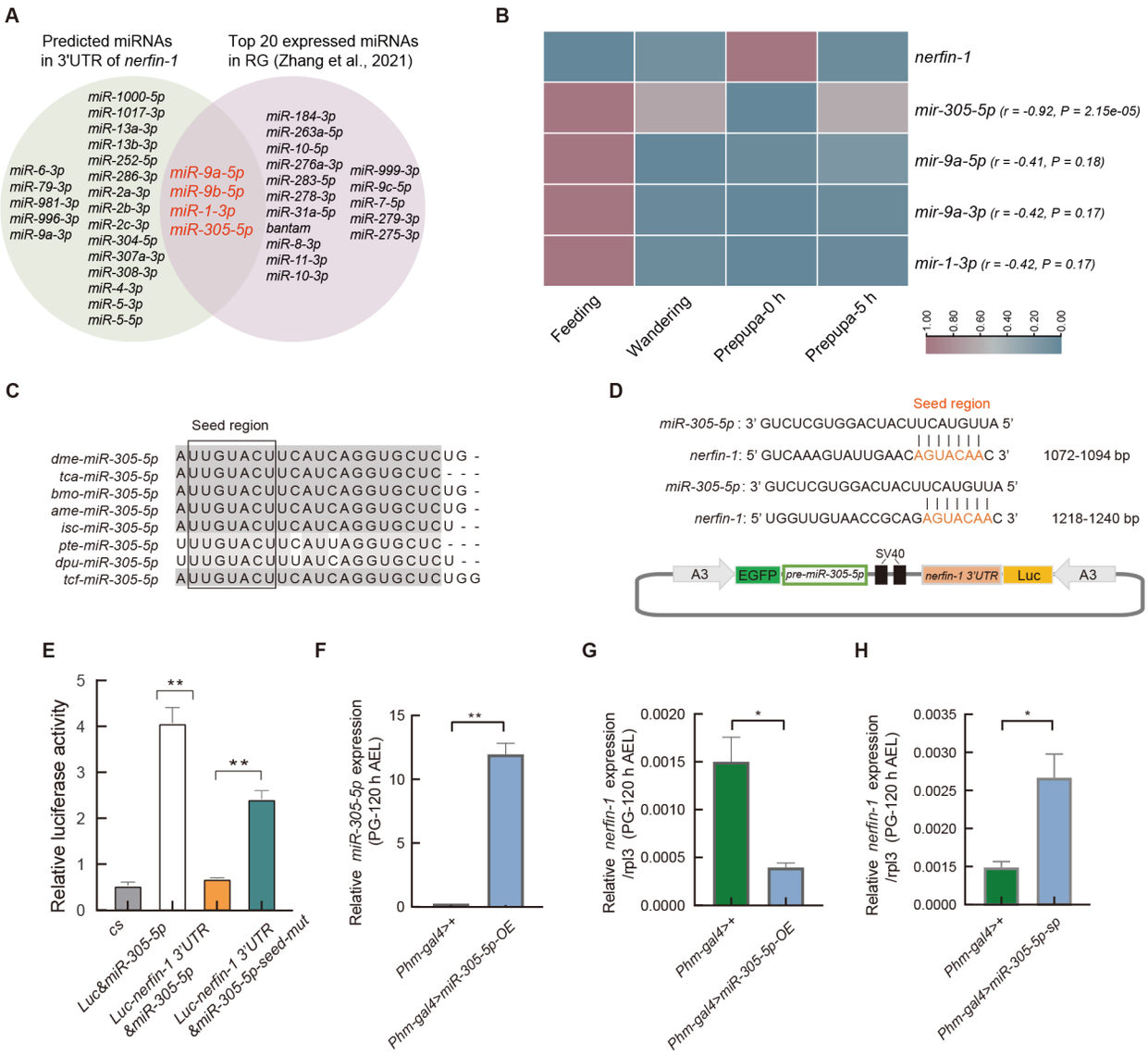

Figure 4 *miR-305-5p* regulates *nerfin-1* expression

A: Identification of potential miRNAs (red) targeting the *nerfin-1* 3′ UTR by intersecting TargetScanFly-predicted miRNAs for the *nerfin-1* 3′ UTR (green circle) with the 20 most highly expressed miRNAs in the ring gland reported previously (purple circle) (Zhang et al., 2021). B: Heatmap showing expression patterns of *nerfin-1* and potential miRNAs. Values are average expression levels obtained from qPCR. Pearson correlation coefficients (*r*) and *P* values between each miRNA and the *nerfin-1* expression pattern are shown. C: Sequence alignment of *miR-305-5p* across arthropod species from miRBase. dme: *D. melanogaster*; tca: *Tribolium castaneum*; bmo: *Bombyx mori*; ame: *Apis mellifera*; isc: *Ixodes scapularis*; pte: *Parasteatoda tepidariorum*; dpu: *Daphnia pulex*; tcf: *Triops cancriformis*. Black box indicates the miRNA seed region. D: Predicted *miR-305-5p* target sites in the *nerfin-1* 3′ UTR. Seed-matched regions are highlighted in red. Lower panel shows dual-luciferase reporter design, including an *actin 3* (*A3*) promoter driving precursor *miR-305-5p* (*pre-miR-305-5p*) expression and *A3* promoter driving firefly *luciferase* (*LUC*) fused to the *nerfin-1* 3′ UTR. E: Relative luciferase activity in dual-luciferase assay. Cs represents blank control without luciferase plasmid. Firefly luciferase activity was normalized against *Renilla* luciferase activity. F: Expression level of *miR-305-5p* in PG cells from control and *miR-305-5p*-overexpressing larvae at 120 h after egg laying (AEL). G: Expression level of *nerfin-1* in PG cells from control and *miR-305-5p*-overexpressing larvae at 120 h AEL. H: Expression level of *nerfin-1* in PG cells from control and *miR-305-5p* sponge (sp)-overexpressing larvae at 120 h AEL. Significance was calculated using Student's *t*-test (*: $P<0.05$; **: $P<0.01$).

specific overexpression of a *miR-305-5p* sponge, which induced miRNA loss-of-function, did not produce obvious developmental abnormalities (Supplementary Figure S4A). In contrast, PG-specific overexpression of *miR-305-5p* caused a significant larval developmental delay (Figure 5A, B). Consistent with the effects of *nerfin-1* RNAi, *miR-305-5p* overexpression down-regulated several *Halloween* genes (Figure 5C, D) and markedly increased *cyp18a1* expression (Figure 5E). Ecdysteroid titers were correspondingly reduced in *miR-305-5p*-overexpressing animals, accompanied by decreased expression of hormone-responsive genes (Figure 5F, G). Dietary 20E supplementation effectively rescued the developmental delay induced by *miR-305-5p* overexpression (Supplementary Figure S4B). Furthermore, *cyp18a1* knockdown in *miR-305-5p*-overexpressing animals restored ecdysteroid titers and significantly advanced pupation timing (Figure 5F, G). Collectively, these results suggest that miR-305-5p regulates ecdysteroid titers by inhibiting nerfin-1, thereby relieving repression of cyp18a1 and promoting ecdysteroid clearance during metamorphic development.

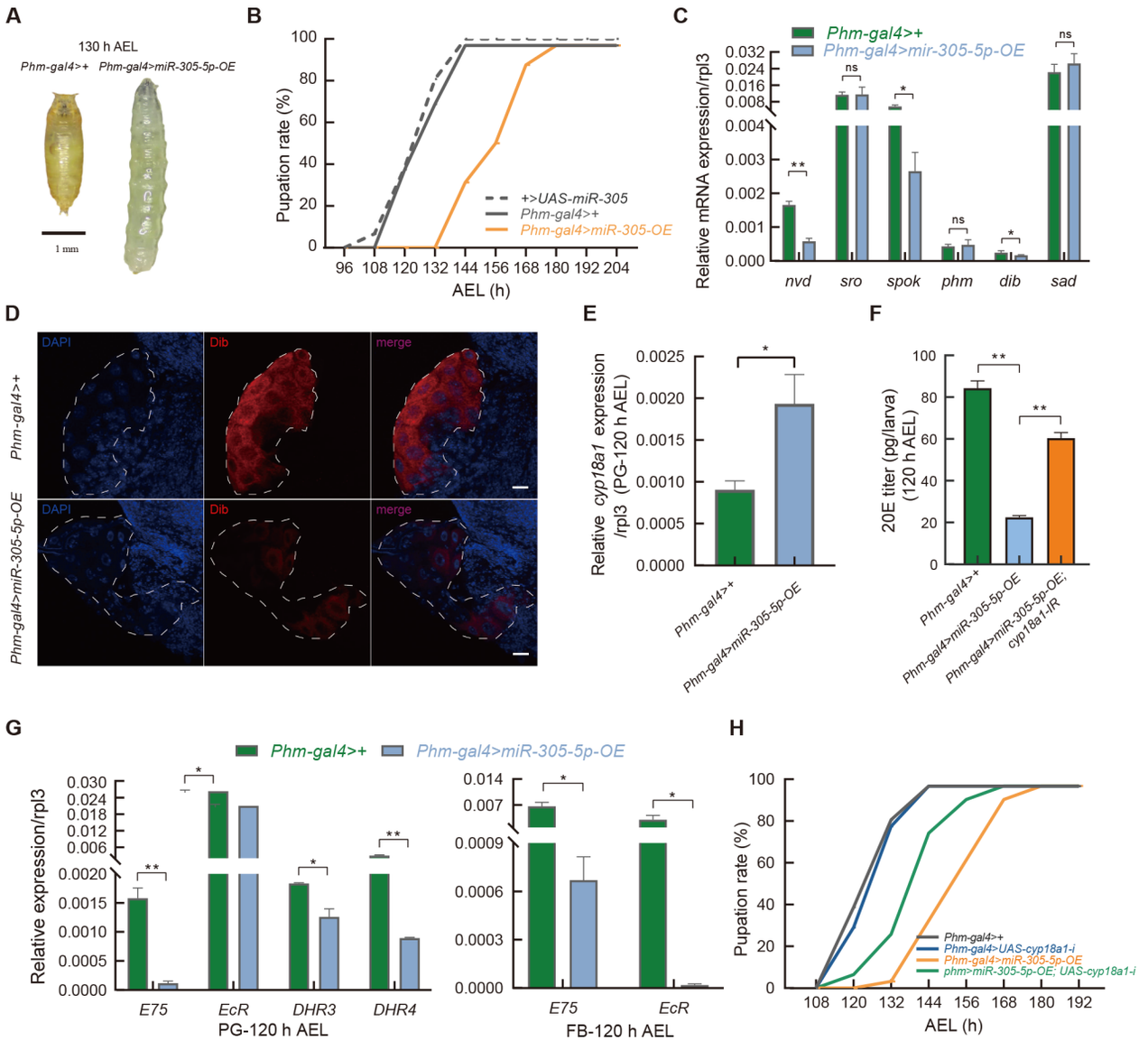

Figure 5 ***miR-305-5p*** **regulates ecdysteroid homeostasis through** ***nerfin-1***

A: PG-specific *miR-305-5p* overexpression caused substantial developmental delay. B: Developmental progression of control (*Phm-gal4>+*) and *miR-305-5p*-overexpressing (*Phm-gal4>miR-305-5p-OE*) larvae. C: Expression of *Halloween* genes in control and *miR-305-5p*-overexpressing larvae at 120 h after egg laying (AEL). D: Immunostaining analysis of Dib protein expression in PG cells from control and *miR-305-5p*-overexpressing larvae at 120 h AEL. Scale bar: 50 μm. E: Expression of *cyp18a1* in control and *miR-305-5p*-overexpressing larvae at 120 h AEL. F: 20E concentrations in control, *miR-305-5p*-overexpressing, and *cyp18a1* RNAi-rescued (*Phm-gal4>miR-305-5p-OE; UAS-cyp18a1-i*) larvae. G: Expression of hormone-responsive genes in ring glands (left panel) and fat bodies (right panel) from control and *miR-305-5p*-overexpressing larvae at 120 h AEL. H: Pupation ratios of *miR-305-5p*-overexpressing and *cyp18a1* RNAi-rescued larvae. Significance was calculated using Student's *t*-test (ns: Not significant; *: $P<0.05$; **: $P<0.01$).

DISCUSSION

Steroid hormone pulses time major developmental transitions in insects, including the larval-to-pupal transition. Transcriptional programs that drive 20E biosynthesis, particularly during pulse initiation and ascent, have been extensively characterized, whereas the molecular mechanisms that promote rapid hormone decline remain less clearly defined (Rewitz et al., 2010). This study identified a novel regulatory axis centered on the transcription factor Nerfin-1 and its upstream regulator *miR-305-5p* that controls ecdysteroid catabolism, thereby shaping pulse termination and supporting developmental fidelity.

Timely reduction of active ecdysteroid levels is required not only to terminate hormone signaling but also to define the duration of endocrine action during development (Lafont et al., 2005). In *Drosophila*, C26 hydroxylation mediated by the cytochrome P450 enzyme Cyp18a1 represents a primary metabolic pathway for ecdysteroid catabolism and inactivation (Guittard et al., 2011; Lafont et al., 2005; Rewitz et al., 2010). Although *cyp18a1* is expressed in multiple ecdysone-responsive tissues, including the salivary glands and fat body, as well as in the hormone-producing PG (Guittard et al., 2011), its regulation in the PG is particularly critical. Both *cyp18a1* overexpression and knockdown in the PG result in lethality, indicating that development requires tight control of this catabolic enzyme (Guittard et al., 2011; Rewitz et al., 2010). The present study found that Nerfin-1 provides this control by repressing *cyp18a1* expression in the PG (Figure 6).

Previous studies have shown that Nerfin-1 binds the

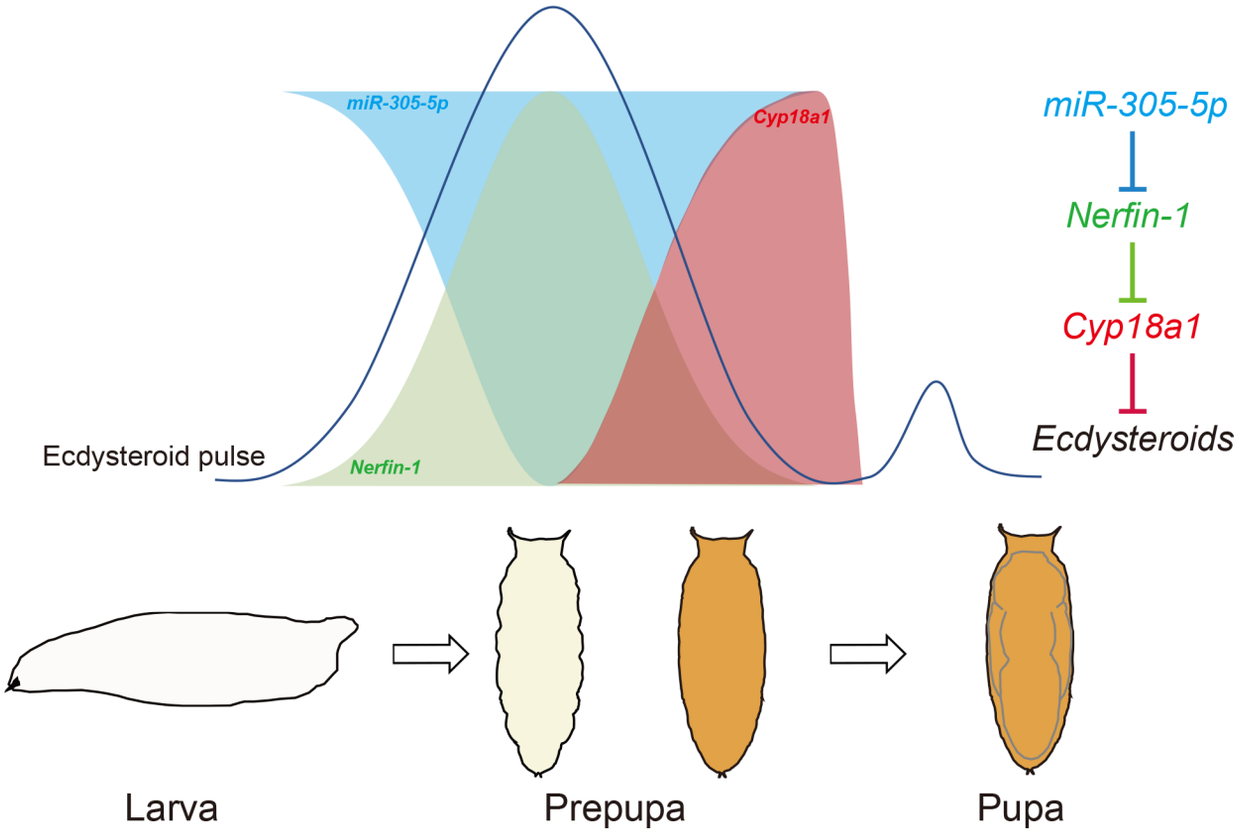

Figure 6 Working model for regulation of the 20E pulse by the *miR-305-5p*/Nerfin-1/Cyp18a1 axis during larval pupation in *Drosophila*

Blue, green, and red curves represent *miR-305-5p*, *nerfin-1*, and *cyp18a1* expression patterns, respectively. Lower panel illustrates developmental progression from the larval stage to the prepupal and pupal stages.

transcriptional enhancer associate domain (TEAD) of Scalloped (Sd) and recruits corepressors such as CtBP and histone deacetylase-associated repressive complexes, thereby promoting chromatin condensation around Sd binding sites to suppress target gene expression (Guo et al., 2019; Vissers et al., 2018). Nerfin-1 and its mammalian ortholog INSM1 can also bind directly to conserved GGGG-containing motifs within gene regulatory regions to modulate transcription (Breslin et al., 2002; Jia et al., 2015; Liu et al., 2006; Wang et al., 2008). In the *Drosophila* PG, Nerfin-1 directly bound to a GGGG motif within the *cyp18a1* regulatory region and acted as a stage-specific repressor. Nerfin-1 expression peaked when ecdysteroid titers were high, from wandering larvae to white prepupae, thereby restraining *cyp18a1* expression and preserving hormone levels during this developmental window. After this stage, declining Nerfin-1 expression relieved repression and permitted Cyp18a1-mediated hormone degradation (Figure 6). This repression is most relevant when hormone titers are sufficient to induce *cyp18a1*, as occurs during late third-instar and prepupal stages (Hurban & Thummel, 1993; Li et al., 2016; Williams et al., 2000). In contrast, in early third-instar larvae, low hormone titers likely keep *cyp18a1* at basal levels without the need for strong transcriptional repression. Interestingly, this regulatory circuit was also detected in the fat body, a major ecdysteroid-responsive tissue. However, fat body-specific *nerfin-1* knockdown caused no apparent developmental defects, consistent with the nonessential role of *cyp18a1* in this tissue and the critical function of *cyp18a1* in the PG (Guittard et al., 2011; Rewitz et al., 2010). Thus, although the Nerfin-1/Cyp18a1 axis operates across multiple tissues, its physiological importance is highly tissue-specific, with *cyp18a1* serving as a critical effector of endocrine timing primarily in the hormone-synthesizing PG.

Although Nerfin-1/INSM1 can function as a transcriptional activator in specific cellular contexts (Chen et al., 2015), and the transcriptomic data from this study revealed that *nerfin-1* knockdown reduced the expression of several genes, including steroidogenic enzymes, multiple lines of evidence suggest that transcriptional activation is unlikely to represent the principal role of Nerfin-1 in the PG. Here, simultaneous knockdown of *nerfin-1* and *cyp18a1* successfully restored ecdysteroid titers, demonstrating that PG steroidogenic capacity remained largely intact in the absence of *nerfin-1*. This suggests that reduced expression of biosynthetic genes occurred as a secondary effect rather than as a direct consequence of loss of a putative Nerfin-1 activator function. The primary defect instead appears to stem from disrupted endocrine homeostasis. The PG functions as both the source of ecdysteroid production and a tissue responsive to ecdysteroid signaling. Therefore, the decline in hormone levels caused by *cyp18a1* derepression following *nerfin-1* knockdown likely weakened the positive-feedback mechanism through which ecdysteroids reinforce expression of biosynthetic enzymes and establish the high hormone titers required for pupariation (Moeller et al., 2013). In this context, reduced *Halloween* gene expression is more consistent with a downstream consequence of diminished hormone signaling than with direct loss of transcriptional activation by Nerfin-1.

Precise temporal control of *nerfin-1* expression is essential for correct *Drosophila* development and is not governed solely by transcriptional regulation (Kuzin et al., 2007). This study identified *miR-305-5p* as an upstream regulator that modulates ecdysteroid degradation by targeting *nerfin-1*,

thereby relieving repression of *cyp18a1* (Figure 6). Through this pathway, developing animals maintain appropriate ecdysteroid levels during the larval-to-pupal transition. The interaction between *miR-305-5p* and *nerfin-1* is consistent with previous evidence that *nerfin-1* mRNA undergoes complex spatiotemporal regulation by multiple miRNAs during nervous system development (Kuzin et al., 2007). These findings suggest that miRNA-mediated repression of *nerfin-1* represents a conserved strategy across tissues, not only to control neuronal differentiation but also to fine-tune endocrine signaling. By targeting *nerfin-1* in the PG, *miR-305-5p* indirectly influences ecdysteroid turnover, extending its regulatory function beyond neural development to systemic endocrine control. More broadly, *miR-305-5p* has emerged as a pleiotropic regulator in *Drosophila*. It was first characterized as a modulator of insulin and Notch signaling in intestinal stem cells, where it supports gut homeostasis under stress conditions (Foronda et al., 2014). Subsequent studies revealed that *miR-305-5p* contributes to aging by targeting mRNAs involved in cellular maintenance (Ueda et al., 2018) and regulates metabolic adaptation during starvation by modulating the activity of the *Drosophila* homolog of p53 (Dp53) in the fat body (Barrio et al., 2014). Together, these findings suggest that *miR-305-5p* functions as a context-dependent integrator of nutritional, hormonal, and developmental signals.

In conclusion, this study established the *miR-305-5p*/Nerfin-1/Cyp18a1 axis as a critical module that fine-tunes ecdysteroid hormone pulses during *Drosophila* metamorphosis. This regulatory cascade coordinates the precise rise and decline of hormone titers required for orderly progression through the complex morphological events of metamorphosis. Disruption of this axis disturbs hormone dynamics, leading to developmental asynchrony and maturation failure, highlighting its fundamental role in robust developmental timing. Intriguingly, the potential relevance of this pathway may extend beyond insects. INSM1, the mammalian homolog of Nerfin-1, is expressed in neuroendocrine cells, including adrenal gland cells, and its deletion severely impairs catecholamine biosynthesis and secretion (Lan & Breslin, 2009; Wildner et al., 2008). This striking parallel raises the possibility that Nerfin-1/INSM1 proteins may contribute to endocrine homeostasis across animal lineages by coordinating hormone production with hormone clearance. Future comparative studies will help determine whether this regulatory principle represents a conserved mechanism for stabilizing endocrine transitions across diverse developmental systems.

DATA AVAILABILITY

The transcriptomic data generated in this study were submitted to the NCBI GEO database (BioProjectID PRJNA1466052), GSA database (accession number PRJCA064240), and Science Data Bank (doi: 10.57760/sciencedb.j00139.00297).

SUPPLEMENTARY DATA

Supplementary data to this article can be found online.

COMPETING INTERESTS

The authors declare that they have no competing interests.

AUTHORS' CONTRIBUTIONS

C.C. performed experiments and bioinformatic analyses, designed figures and contributed to manuscript writing. Z.Z. supervised the project, designed the experiment, and contributed to manuscript writing. W.S. conceptualized the project, designed the experiment, supervised the project, contributed to funding acquisition, and revised the manuscript. All authors read and approved the final version of the manuscript.

ACKNOWLEDGMENTS

We greatly appreciate the help and advice from members of our lab. We also thank Shijiang Qin from Chongqing University for assistance with the hormone titer assays.

REFERENCES

Agarwal V, Subtelny A, Thiru P, et al. 2018. Predicting microRNA targeting efficacy in *Drosophila*. *Genome Biology*, **19**: 152.

Andres AJ, Thummel CS. 1992. Hormones, puffs and flies: the molecular control of metamorphosis by ecdysone. *Trends in Genetics*, **8**(4): 132–138.

Barrio L, Dekanty A, Milán M. 2014. MicroRNA-mediated regulation of Dp53 in the *Drosophila* fat body contributes to metabolic adaptation to nutrient deprivation. *Cell Reports*, **8**(2): 528–541.

Boulan L, Martín D, Milán M. 2013. bantam miRNA promotes systemic growth by connecting insulin signaling and ecdysone production. *Current Biology*, **23**(6): 473–478.

Breslin MB, Zhu M, Notkins AL, et al. 2002. Neuroendocrine differentiation factor, IA-1, is a transcriptional repressor and contains a specific DNA-binding domain: identification of consensus IA-1 binding sequence. *Nucleic Acids Research*, **30**(4): 1038–1045.

Chen C, Breslin MB, Lan MS. 2015. INSM1 increases N-myc stability and oncogenesis via a positive-feedback loop in neuroblastoma. *Oncotarget*, **6**(34): 36700–36712.

Cheng CC, Ko A, Chaieb L, et al. 2014. The POU factor ventral veins lacking/drifter directs the timing of metamorphosis through ecdysteroid and juvenile hormone signaling. *PLoS Genetics*, **10**(6): e1004425.

Danielsen ET, Moeller ME, Yamanaka N, et al. 2016. A *Drosophila* genome-wide screen identifies regulators of steroid hormone production and developmental timing. *Developmental Cell*, **37**(6): 558–570.

Enya S, Ameku T, Igarashi F, et al. 2014. A Halloween gene *noppera-bo* encodes a glutathione S-transferase essential for ecdysteroid biosynthesis via regulating the behaviour of cholesterol in *Drosophila*. *Scientific Reports*, **4**(1): 6586.

Farkas LM, Haffner C, Giger T, et al. 2008. Insulinoma-associated 1 has a panneurogenic role and promotes the generation and expansion of basal progenitors in the developing mouse neocortex. *Neuron*, **60**(1): 40–55.

Foronda D, Weng RF, Verma P, et al. 2014. Coordination of insulin and Notch pathway activities by microRNA miR-305 mediates adaptive homeostasis in the intestinal stem cells of the *Drosophila* gut. *Genes & Development*, **28**(21): 2421–2431.

Froldi F, Szuperak M, Weng CF, et al. 2015. The transcription factor Nerfin-1 prevents reversion of neurons into neural stem cells. *Genes & Development*, **29**(2): 129–143.

Guittard E, Blais C, Maria A, et al. 2011. CYP18A1, a key enzyme of *Drosophila* steroid hormone inactivation, is essential for metamorphosis. *Developmental Biology*, **349**(1): 35–45.

Guo PF, Lee CH, Lei HY, et al. 2019. Nerfin-1 represses transcriptional output of Hippo signaling in cell competition. *eLife*, **8**: e38843.

He K, Xiao HM, Sun Y, et al. 2019. microRNA-14 as an efficient suppressor to switch off ecdysone production after ecdysis in insects. *RNA Biology*, **16**(9): 1313–1325.

Hodgetts RB, Sage B, O'Connor JD. 1977. Ecdysone titers during postembryonic development of *Drosophila melanogaster*. *Developmental Biology*, **60**(1): 310–317.

Jia SQ, Ivanov A, Blasevic D, et al. 2015. Insm1 cooperates with Neurod1 and Foxa2 to maintain mature pancreatic β-cell function. *The EMBO Journal*, **34**(10): 1417–1433.

Kamiyama T, Niwa R. 2022. Transcriptional regulators of ecdysteroid biosynthetic enzymes and their roles in insect development. *Frontiers in Physiology*, **13**: 823418.

Komura-Kawa T, Hirota K, Shimada-Niwa Y, et al. 2015. The *Drosophila* zinc finger transcription factor Ouija board controls ecdysteroid biosynthesis through specific regulation of *spookier*. *PLoS Genetics*, **11**(12): e1005712.

Kuzin A, Kundu M, Brody T, et al. 2007. The *Drosophila nerfin-1* mRNA requires multiple microRNAs to regulate its spatial and temporal translation dynamics in the developing nervous system. *Developmental Biology*, **310**(1): 35–43.

Lafont R, Dauphin-Villemant C, Warren JT, et al. 2005. Ecdysteroid chemistry and biochemistry. *Comprehensive Molecular Insect Science*, **3**: 125–195.

Lan MS, Breslin MB. 2009. Structure, expression, and biological function of INSM1 transcription factor in neuroendocrine differentiation. *The FASEB Journal*, **23**(7): 2024–2033.

Li K, Tian L, Guo ZJ, et al. 2016. 20-Hydroxyecdysone (20E) primary response gene E75 isoforms mediate steroidogenesis autoregulation and regulate developmental timing in *Bombyx*. *Journal of Biological Chemistry*, **291**(35): 18163–18175.

Lim DH, Lee S, Choi MS, et al. 2020. The conserved microRNA miR‐8‐3p coordinates the expression of V‐ATPase subunits to regulate ecdysone biosynthesis for *Drosophila* metamorphosis. *The FASEB Journal*, **34**(5): 6449–6465.

Liu SN, Li K, Gao Y, et al. 2018. Antagonistic actions of juvenile hormone and 20-hydroxyecdysone within the ring gland determine developmental transitions in *Drosophila*. *Proceedings of the National Academy of Sciences of the United States of America*, **115**(1): 139–144.

Liu W, Yan MY, King-Jones K. 2024. Soul is a master control gene governing the development of the *Drosophila* prothoracic gland. *Proceedings of the National Academy of Sciences of the United States of America*, **121**(40): e2405469121.

Liu WD, Wang HW, Muguira M, et al. 2006. INSM1 functions as a transcriptional repressor of the neuroD/β2 gene through the recruitment of cyclin D1 and histone deacetylases. *Biochemical Journal*, **397**(1): 169–177.

Love MI, Huber W, Anders S. 2014. Moderated estimation of fold change and dispersion for RNA-seq data with DESeq2. *Genome Biology*, **15**(12): 550.

Moeller ME, Danielsen ET, Herder R, et al. 2013. Dynamic feedback circuits function as a switch for shaping a maturation-inducing steroid pulse in *Drosophila*. *Development*, **140**(23): 4730–4739.

Niwa R, Matsuda T, Yoshiyama T, et al. 2004. CYP306A1, a cytochrome P450 enzyme, is essential for ecdysteroid biosynthesis in the prothoracic glands of *Bombyx* and *Drosophila*. *Journal of Biological Chemistry*, **279**(34): 35942–35949.

Niwa R, Namiki T, Ito K, et al. 2010. *Non-molting glossy* / *shroud* encodes a short-chain dehydrogenase/reductase that functions in the 'Black Box' of the ecdysteroid biosynthesis pathway. *Development*, **137**(12): 1991–1999.

Niwa R, Sakudoh T, Namiki T, et al. 2005. The ecdysteroidogenic P450 Cyp302a1/disembodied from the silkworm, *Bombyx mori*, is transcriptionally regulated by prothoracicotropic hormone. *Insect Molecular Biology*, **14**(5): 563–571.

Niwa YS, Niwa R. 2016. Transcriptional regulation of insect steroid hormone biosynthesis and its role in controlling timing of molting and metamorphosis. *Development, Growth & Differentiation*, **58**(1): 94–105.

Ohhara Y, Shimada-Niwa Y, Niwa R, et al. 2015. Autocrine regulation of ecdysone synthesis by β3-octopamine receptor in the prothoracic gland is essential for *Drosophila* metamorphosis. *Proceedings of the National Academy of Sciences of the United States of America*, **112**(5): 1452–1457.

Ono H, Rewitz KF, Shinoda T, et al. 2006. Spook and Spookier code for stage-specific components of the ecdysone biosynthetic pathway in Diptera. *Developmental Biology*, **298**(2): 555–570.

Ou QX, Magico A, King-Jones K. 2011. Nuclear receptor DHR4 controls the timing of steroid hormone pulses during *Drosophila* development. *PLoS Biology*, **9**(9): e1001160.

Parvy JP, Blais C, Bernard F, et al. 2005. A role for βFTZ-F1 in regulating ecdysteroid titers during post-embryonic development in *Drosophila melanogaster*. *Developmental Biology*, **282**(1): 84–94.

Parvy JP, Wang P, Garrido D, et al. 2014. Forward and feedback regulation of cyclic steroid production in *Drosophila melanogaster*. *Development*, **141**(20): 3955–3965.

Pertea M, Kim D, Pertea GM, et al. 2016. Transcript-level expression analysis of RNA-seq experiments with HISAT, StringTie and Ballgown. *Nature Protocols*, **11**(9): 1650–1667.

Petryk A, Warren JT, Marqués G, et al. 2003. Shade is the *Drosophila* P450 enzyme that mediates the hydroxylation of ecdysone to the steroid insect molting hormone 20-hydroxyecdysone. *Proceedings of the National Academy of Sciences of the United States of America*, **100**(24): 13773–13778.

Rewitz KF, Yamanaka N, Gilbert LI, et al. 2009. The insect neuropeptide PTTH activates receptor tyrosine kinase torso to initiate metamorphosis. *Science*, **326**(5958): 1403–1405.

Rewitz KF, Yamanaka N, O'Connor MB. 2010. Steroid hormone inactivation is required during the juvenile-adult transition in *Drosophila*. *Developmental Cell*, **19**(6): 895–902.

Rewitz KF, Yamanaka N, O'Connor MB. 2013. Developmental checkpoints and feedback circuits time insect maturation. *Current Topics in Developmental Biology*, **103**: 1–33.

Riddiford LM, Hiruma K, Zhou XF, et al. 2003. Insights into the molecular basis of the hormonal control of molting and metamorphosis from *Manduca sexta* and *Drosophila melanogaster*. *Insect Biochemistry and Molecular Biology*, **33**(12): 1327–1338.

Sewe SO, Silva G, Sicat P, et al. 2022. Trimming and validation of Illumina short reads using trimmomatic, trinity assembly, and assessment of RNA-Seq data. *In*: Edwards D. Plant Bioinformatics: Methods and Protocols. New York: Humana, 211–232.

Sherman BT, Hao M, Qiu J, et al. 2022. DAVID: a web server for functional enrichment analysis and functional annotation of gene lists (2021 update). *Nucleic Acids Research*, **50**(W1): W216–W221.

Tennessen J, Thummel C. 2011. Coordinating growth and maturation—insights from *Drosophila*. *Current Biology*, **21**(18): R750–R757.

Terasawa E, Fernandez DL. 2001. Neurobiological mechanisms of the onset of puberty in primates. *Endocrine Reviews*, **22**(1): 111–151.

Ueda M, Sato T, Ohkawa Y, et al. 2018. Identification of *miR-305*, a microRNA that promotes aging, and its target mRNAs in *Drosophila*. *Genes to Cells*, **23**(2): 80–93.

Uryu O, Ou QX, Komura-Kawa T, et al. 2018. Cooperative control of ecdysone biosynthesis in *Drosophila* by transcription factors Séance, Ouija Board, and Molting Defective. *Genetics*, **208**(2): 605–622.

Vissers JHA, Froldi F, Schröder J, et al. 2018. The Scalloped and Nerfin-1 transcription factors cooperate to maintain neuronal cell fate. *Cell Reports*, **25**(6): 1561–1576. e7.

Wang HW, Muguira M, Liu WD, et al. 2008. Identification of an INSM1-binding site in the insulin promoter: negative regulation of the insulin gene transcription. *Journal of Endocrinology*, **198**(1): 29–39.

Warren JT, Yerushalmi Y, Shimell MJ, et al. 2006. Discrete pulses of molting hormone, 20-hydroxyecdysone, during late larval development of *Drosophila melanogaster*: correlations with changes in gene activity. *Developmental Dynamics*, **235**(2): 315–326.

Wildner H, Gierl MS, Strehle M, et al. 2008. Insm1 (IA-1) is a crucial component of the transcriptional network that controls differentiation of the sympatho-adrenal lineage. *Development*, **135**(3): 473–481.

Wu J, Duggan A, Chalfie M. 2001. Inhibition of touch cell fate by *egl-44* and *egl-46* in *C. elegans*. *Genes & Development*, **15**(6): 789–802.

Xu JJ, Hao X, Yin MX, et al. 2017. Prevention of medulla neuron dedifferentiation by Nerfin-1 requires inhibition of Notch activity. *Development*, **144**(8): 1510–1517.

Xue XY, Liu ZH, Zhang Z, et al. 2025. Cullin1 orchestrates insulin/mTOR signaling to drive endocycle progression and ecdysteroid production in *Drosophila* prothoracic glands during critical weight attainment. *Insect Biochemistry and Molecular Biology*, **183**: 104374.

Yamanaka N, Hua YJ, Mizoguchi A, et al. 2005. Identification of a novel prothoracicostatic hormone and its receptor in the silkworm *Bombyx mori*. *Journal of Biological Chemistry*, **280**(15): 14684–14690.

Yamanaka N, Rewitz KF, O'Connor MB. 2013. Ecdysone control of developmental transitions: lessons from *Drosophila* research. *Annual Review of Entomology*, **58**(1): 497–516.

Yoshiyama T, Namiki T, Mita K, et al. 2006. Neverland is an evolutionally conserved Rieske-domain protein that is essential for ecdysone synthesis and insect growth. *Development*, **133**(13): 2565–2574.

Zeng J, Huynh N, Phelps B, et al. 2020. Snail synchronizes endocycling in a TOR-dependent manner to coordinate entry and escape from endoreplication pausing during the *Drosophila* critical weight checkpoint. *PLoS Biology*, **18**(2): e3000609.

Zhang J, Wen D, Li EY, et al. 2021. MicroRNA miR-8 promotes cell growth of corpus allatum and juvenile hormone biosynthesis independent of insulin/IGF signaling in *Drosophila melanogaster*. *Insect Biochemistry and Molecular Biology*, **136**: 103611.

Zhang TL, Song W, Li Z, et al. 2018. Krüppel homolog 1 represses insect ecdysone biosynthesis by directly inhibiting the transcription of steroidogenic enzymes. *Proceedings of the National Academy of Sciences of the United States of America*, **115**(15): 3960–3965.

Zhou H, He XL, Xiong Y, et al. 2025. Structural insights into a highly flexible zinc finger module unravel INSM1 function in transcription regulation. *Nature Communications*, **16**(1): 2162.